THE ASTROPHYSICAL JOURNAL, 405:685–697, 1993 March 10

BEYOND CLAUSIUS-MOSSOTTI: WAVE PROPAGATION ON A POLARIZABLE POINT LATTICE AND THE DISCRETE DIPOLE APPROXIMATION

B. T. DRAINE[1] AND JEREMY GOODMAN[2]
Princeton University Observatory, Peyton Hall, Princeton, NJ 08544
Received 1992 June 12; accepted 1992 September 17

ABSTRACT

We derive the dispersion relation for electromagnetic waves propagating on a lattice of polarizable points. From this dispersion relation we obtain a prescription for choosing dipole polarizabilities so that an infinite lattice with finite lattice spacing will mimic a continuum with dielectric constant $\epsilon(\omega)$. The Discrete Dipole Approximation is used to calculate scattering and absorption by a finite target by replacing the target with an array of point dipoles. We compare different prescriptions for determining the dipole polarizabilities. We show that the most accurate results are obtained when the lattice dispersion relation is used to set the polarizabilities.

Subject headings: dust, extinction — polarization

1. INTRODUCTION

Several different numerical techniques have been proposed for approximate calculation of scattering and absorption of electromagnetic waves by irregular objects such as interstellar grains. Finite element methods, in particular, are quite attractive, since they may be easily adapted to different target geometries.

The "Discrete-Dipole Approximation" (DDA) is a finite element method in which the continuum target is replaced by an array of point dipoles (Purcell & Pennypacker 1973; Draine 1988); the scattering problem is then solved for this dipole array. The DDA has been applied to a variety of problems, including calculations of the properties of magnetite grains (Shapiro 1975), graphite grains (Draine 1988), "graphitic onions" (Wright 1988), NH_3 tetrahedra (West et al. 1989), and fractal grains (West 1991; Hawkins & Wright 1992; Kozasa, Blum, & Mukai 1992). The power of the DDA has recently been greatly enhanced by the application of Fast Fourier Transform methods (Goodman, Draine, & Flatau 1991); solution of scattering problems using arrays of 10^4–10^5 dipoles is now feasible.

In order to calculate scattering and absorption by a continuum target of dielectric constant $\epsilon(\omega)$, the DDA requires a prescription for determining the polarizabilities $\alpha(\omega)$ of the point dipoles used to represent the target. In the "static" limit $\omega d/c \rightarrow 0$ (where d is the lattice spacing) the Clausius-Mossotti relation gives the effective dielectric constant $\epsilon(\omega)$ of a cubic lattice of points with polarizability $\alpha(\omega)$. Purcell & Pennypacker (1973) used the Clausius-Mossotti relation to set the dipole polarizabilities; Draine (1988) improved upon this by adding a radiative reaction correction term.

A closely related technique, originally proposed by Livesay & Chen (1974), is referred to as the "Digitized Green's Function" (DGF) method (Goedecke & O'Brien 1988), or the "Volume Integral Equation Formulation" (VIEF) method (Hage, Greenberg, & Wang 1991). The DGF and VIEF methods, as implemented by Goedecke & O'Brien (1988) and Hage & Greenberg (1990), are in fact identical. As has been shown (Hage & Greenberg 1990), the DGF/VIEF method is itself mathematically equivalent to the DDA, departing only in use of a different prescription for choosing the dipole polarizabilities. Hage & Greenberg (1990) showed that for the cases they considered, the DGF/VIEF prescription for the dipole polarizabilities generally gave better results than that used by Draine (1988).

Since DDA results depend directly upon the dipole polarizabilities, it is important to determine the optimal method for choosing them.

In this paper we seek to establish, from first principles, the "best" prescription for the dipole polarizabilities by solving a closely related problem: choosing the dipole polarizabilities such that an *infinite* lattice of point dipoles will propagate electromagnetic plane waves with the same dispersion relation as a medium of specified dielectric function ϵ. In effect, we seek to extend the Clausius-Mossotti relation to the physically interesting case of $\omega d/c \neq 0$.

The DDA is briefly reviewed in § 2. In § 3 we obtain the lattice dispersion relation ("LDR") for electromagnetic waves propagating on an infinite cubic lattice of point dipoles of polarizability α and lattice spacing d. In § 4 we examine the LDR in the long-wavelength limit; by requiring that the lattice reproduce the dispersion relation of a continuum medium with dielectric function $\epsilon(\omega)$, we obtain a condition determining the dipole polarizability $\alpha(\epsilon, k_0 d)$ including terms up to $O[(k_0 d)^3]$, where $k_0 \equiv \omega/c$ is the wave vector in vacuo.

In order to compare our new prescription for α with those proposed previously, in § 5 we report the results of extensive DDA calculations for absorption and scattering by homogeneous spheres, and we compare exact Mie theory results with DDA calculations using four different prescriptions for α. We find that for $|\epsilon - 1| \lesssim 5$ the LDR-based prescription for the dipole polarizabilities generally provides more accurate results for scattering and absorption by spheres; this superiority is presumed to extend to

[1] E-mail: draine@astro.princeton.edu.
[2] E-mail: jeremy@astro.princeton.edu.

nonspherical and inhomogeneous targets. For larger values of $|\epsilon - 1|$ the different prescriptions tend to provide comparable accuracy.

We conclude that DDA calculations of absorption and scattering by arbitrary targets should use the LDR-based prescription for the dipole polarizabilities.

2. THE DISCRETE DIPOLE APPROXIMATION

The DDA is a flexible technique for calculating scattering and absorption of electromagnetic waves by an arbitrary object (Purcell & Pennypacker 1973; Draine 1988). The target is approximated by an array of N point dipoles at positions $\boldsymbol{r}_i$ with polarizabilities $\boldsymbol{\alpha}_i$. The polarization

$$\boldsymbol{P}_i = \boldsymbol{\alpha}_i \cdot \boldsymbol{E}(\boldsymbol{r}_i) \tag{2.1}$$

of each dipole responds to the total electric field at its position; $\boldsymbol{E}(\boldsymbol{r}_i)$ is the sum of an incident plane wave

$$\boldsymbol{E}_{\mathrm{inc},i} = \boldsymbol{E}_0 \exp(i\boldsymbol{k}_0 \cdot \boldsymbol{r}_i - i\omega t) \tag{2.2}$$

and a contribution from all of the other dipoles,

$$\boldsymbol{E}_{\mathrm{other},i} = -\sum_{j\neq i} \boldsymbol{A}_{ij} \cdot \boldsymbol{P}_j \ . \tag{2.3}$$

Here $\boldsymbol{k}_0$ is the propagation vector in vacuo ($|\boldsymbol{k}_0| = \omega/c$). Thus,

$$(\boldsymbol{\alpha}_i)^{-1}\boldsymbol{P}_i + \sum_{j\neq i} \boldsymbol{A}_{ij} \cdot \boldsymbol{P}_j = \boldsymbol{E}_{\mathrm{inc},i} \ . \tag{2.4}$$

Since $\boldsymbol{E}_{\mathrm{inc},i}$ and $\boldsymbol{P}_i$ are three-dimensional vectors, the matrix $\boldsymbol{A}$ can be thought of as a symmetric $N \times N$ array of 3×3 tensors (see Draine 1988). Note that for anisotropic media, the polarizabilities $\boldsymbol{\alpha}_i$ will be 3×3 tensors.

The scattering problem for the array of point dipoles, represented by the system of linear equations (2.4), can be solved to arbitrary accuracy; it has recently been shown that FFT techniques, together with the conjugate gradient method, can be used to obtain solutions for targets represented by $N > 10^5$ dipoles (Goodman, Draine, & Flatau 1991).

Representation of a continuum target by a dipole array requires prescriptions for (1) the locations of the point dipoles and (2) the individual dipole polarizabilities $\boldsymbol{\alpha}_i$. FFT techniques require the dipoles to be located on a lattice; here we will restrict attention to the simplest choice: a cubic lattice.

We specify the "occupied" lattice sites using the following simple approach: given a continuum target of volume V, we set up a trial lattice of lattice spacing d_0, position the lattice relative to the target shape, and identify the N lattice sites which are located within the volume V.[3] With these N occupied lattice sites now determined, we then slightly adjust the lattice spacing to be $d = (V/N)^{1/3}$ so that the target volume is equal to the volume of N unit cells. An important dimensionless number characterizing the electromagnetic response of the array will be the product $k_0 d$—the change in phase of the wave (in vacuo) corresponding to the lattice spacing.

The continuum medium is characterized by its complex dielectric function ϵ, or its complex refractive index $m = \epsilon^{1/2}$. In the limit $k_0 d \to 0$, the dipole polarizabilities $\boldsymbol{\alpha}_i$ must be given by the "Clausius-Mossotti" polarizability (e.g., Jackson 1975)

$$\boldsymbol{\alpha}_i^{(0)} \equiv \frac{3d^3}{4\pi}\left(\frac{m_i^2 - 1}{m_i^2 + 2}\right), \tag{2.5}$$

where m_i is the refractive index at lattice site i.[4] Using the optical theorem, Draine (1988) showed that when $k_0 d$ was finite the polarizabilities α_i should include a radiative-reaction correction:

$$\boldsymbol{\alpha}_i = \frac{\boldsymbol{\alpha}_i^{(nr)}}{1 - (2/3)i(\boldsymbol{\alpha}_i^{(nr)}/d^3)(k_0 d)^3}, \tag{2.6}$$

where the "nonradiative" polarizability $\boldsymbol{\alpha}_i^{(nr)}$ is the polarizability in the *absence* of the radiative reaction correction. This formal separation of the radiative-reaction correction from possible other corrections in $\boldsymbol{\alpha}_i^{(nr)}$ ensures that the DDA solutions rigorously satisfy the optical theorem (Draine 1988).

The present paper examines and compares different choices for $\boldsymbol{\alpha}_i^{(nr)}$. Draine (1988) used

$$\boldsymbol{\alpha}_i^{(nr)} \approx \boldsymbol{\alpha}_i^{(0)}, \tag{2.7}$$

which we shall refer to as "Clausius-Mossotti plus radiative reaction" (CMRR).

Goedecke & O'Brien (1988) and Hage & Greenberg (1990) showed that the fundamental DDA equation (2.4) can be derived from a simple discretization of an integral formulation of the scattering problem: the "DGF/VIEF" method. These authors concluded

[3] Normally one would position the lattice so that the target centroid $(x_c, y_c, z_c) = (n_x, n_y, n_z)d/2$, where n_x, n_y, and n_z are all integers; otherwise target symmetries (e.g., under x-reflection) would not be present in the array. The decision on whether to use even or odd n_x must be based on geometric criteria which we do not discuss here.

[4] In the case of an anisotropic material, eq. (2.5) applies in the coordinate system where the tensor $\epsilon = m^2$ is diagonalized; $\boldsymbol{\alpha}_i^{(0)}$ is then also diagonal, and eq. (2.5) then relates the diagonal elements of $\boldsymbol{\alpha}_i^{(0)}$ to the diagonal elements of ϵ.

that the dipole polarizabilities should be given by

$$\alpha_i \approx \frac{\alpha^{(0)}}{1 + (\alpha_i^{(0)}/d^3)[b_1(k_0 d)^2 - (2/3)i(k_0 d)^3]} , \tag{2.8}$$

or, to the same order of accuracy, the "nonradiative" polarizability is

$$\alpha_i^{(nr)} = \frac{\alpha_i^{(0)}}{1 + (\alpha_i^{(0)}/d^3)b_1(k_0 d)^2} , \tag{2.9}$$

where

$$b_1 = -(4\pi/3)^{1/2} = -1.611992 \ldots . \tag{2.10}$$

Thus Goedecke & O'Brien (1988) and Hage & Greenberg (1990) recommend use of an $O[(k_0 d)^2]$ correction. Unfortunately, in their derivation of (2.8), these authors assumed that the electric field $\boldsymbol{E}$ could be approximated as uniform over regions of volume d^3; this assumption introduces errors of order $(k_0 d)^2$, so that the result (2.8) is suspect. Nevertheless, it was shown by Hage & Greenberg that use of equation (2.9) could increase the accuracy of DDA calculations, compared to results obtained with equation (2.7), at least for the cases they tested.

Since it will prove desirable to carry out DDA calculations for $k_0 d \approx 0.5$ or larger, it is of interest to determine rigorously the $O[(k_0 d)^2]$ and $O[(k_0 d)^3]$ corrections to the dipole polarizabilities. We do so by examining the propagation of an electromagnetic wave on a polarization lattice.

3. WAVE PROPAGATION ON AN INFINITE POLARIZABLE LATTICE

The problem of wave propagation by periodic arrays of finite-size particles has been considered previously (Ohtaka 1979; Waterman & Pedersen 1986). Here we shall restrict attention to polarizable *points* on a lattice—this being precisely the case of interest for the DDA. For this case we shall see that the dispersion relation for the lattice can be solved exactly (eq. [3.15]–[3.20] below). By further restricting attention to the limit where the wavelength is large compared to the lattice spacing, we shall find in § 4 that various integrals which appear in the exact dispersion relation may be evaluated analytically.

Consider an infinite cubic lattice. At each lattice site $\boldsymbol{x}_n = \boldsymbol{n}d$ [where $\boldsymbol{n} = (i, j, k)$] is located a dipole with polarizability α and dipole moment $\boldsymbol{P}_n$ given by equations (2.1)–(2.4). We will take the polarizability α to be scalar, so that in the limit $k_0 d \rightarrow 0$ this lattice will approximate an isotropic medium. If we assume $\boldsymbol{P}_n(t) = \boldsymbol{P}_0(0)e^{i\boldsymbol{k}\cdot\boldsymbol{n}d - i\omega t}$ and adopt the Lorentz gauge condition

$$\nabla \cdot \boldsymbol{A} + \frac{1}{c}\frac{\partial \Phi}{\partial t} = 0 , \tag{3.1}$$

then the vector potential $\boldsymbol{A}(\boldsymbol{x}, t)$ satisfies the wave equation

$$\nabla^2 \boldsymbol{A} + \frac{\omega^2}{c^2}\boldsymbol{A} = -\frac{4\pi}{c}\boldsymbol{J} \tag{3.2}$$

$$= \frac{4\pi i\omega}{c}\sum_{\boldsymbol{n}} \boldsymbol{P}_n \delta^3(\boldsymbol{x} - \boldsymbol{x}_n) \tag{3.3}$$

$$= \frac{4\pi i\omega}{c}\boldsymbol{P}_0 e^{i\boldsymbol{k}\cdot\boldsymbol{x}}\sum_{\boldsymbol{n}} \delta^3(\boldsymbol{x} - \boldsymbol{x}_n) . \tag{3.4}$$

Consider now the unit cell centered on $\boldsymbol{x}_0 = 0$. Let $\boldsymbol{A}_{\rm other}$ and $\Phi_{\rm other}$ be the potentials in this region due to all dipoles *except* the dipole at $\boldsymbol{x} = 0$. Thus

$$\boldsymbol{E}_{\rm other}(\boldsymbol{x}, t) = -\frac{1}{c}\frac{\partial \boldsymbol{A}_{\rm other}}{\partial t} - \nabla\Phi_{\rm other} = \frac{i\omega}{c}\boldsymbol{A}_\perp(\boldsymbol{x}, t) \tag{3.5}$$

where

$$\boldsymbol{A}_\perp(\boldsymbol{x}, t) \equiv \boldsymbol{A}_{\rm other} + \frac{c^2}{\omega^2}\nabla(\nabla \cdot \boldsymbol{A}_{\rm other}) . \tag{3.6}$$

Thus

$$\boldsymbol{P}_0(0) = \frac{\alpha i\omega}{c}\boldsymbol{A}_\perp(\boldsymbol{x} = 0, t = 0) . \tag{3.7}$$

The vector potential can be written

$$\boldsymbol{A}(\boldsymbol{x}, t) = e^{i\boldsymbol{k}\cdot\boldsymbol{x} - i\omega t}\sum_{\boldsymbol{n}} \boldsymbol{a}_n e^{i\boldsymbol{q}_n\cdot\boldsymbol{x}} \tag{3.8}$$

where $q \equiv 2\pi/d$. Then equations (3.4) and (3.8), and the identity $\sum_{\boldsymbol{n}} \delta^3(\boldsymbol{x} - \boldsymbol{n}d) = d^{-3} \sum_{\boldsymbol{n}} e^{iq\boldsymbol{n}\cdot\boldsymbol{x}}$ yield

$$\boldsymbol{a}_{\boldsymbol{n}} = \frac{4\pi\omega^2}{c^2} \frac{\alpha}{d^3} \boldsymbol{A}_\perp(0, 0)\left(|\boldsymbol{k} + q\boldsymbol{n}|^2 - \frac{\omega^2}{c^2}\right)^{-1} . \tag{3.9}$$

The field $\boldsymbol{A}_{\rm self}(\boldsymbol{x}, t)$ due to the dipole at $\boldsymbol{x} = 0$ is

$$\boldsymbol{A}_{\rm self}(\boldsymbol{x}, t) = \frac{-i\omega}{c} \boldsymbol{P}_0 \frac{e^{i\omega r/c}}{r} = \frac{\omega^2}{c^2} \alpha \boldsymbol{A}_\perp(0, 0) \frac{e^{i\omega r/c}}{r} e^{-i\omega t} . \tag{3.10}$$

With the identity

$$\frac{e^{i\omega r/c}}{r} = \frac{e^{i\boldsymbol{k}\cdot\boldsymbol{x}}}{2\pi^2} \int d^3k' \frac{e^{i\boldsymbol{k}'\cdot\boldsymbol{x}}}{|\boldsymbol{k}' + \boldsymbol{k}|^2 - \omega^2/c^2} \tag{3.11}$$

we obtain

$$\boldsymbol{A}_{\rm other} = \frac{4\pi\omega^2}{c^2} \frac{\alpha}{d^3} e^{i\boldsymbol{k}\cdot\boldsymbol{x} - i\omega t} \boldsymbol{A}_\perp(0, 0)\left(\sum_{\boldsymbol{n}} \frac{e^{iq\boldsymbol{n}\cdot\boldsymbol{x}}}{|\boldsymbol{k} + q\boldsymbol{n}|^2 - \omega^2/c^2} - \int \frac{d^3k'}{q^3} \frac{e^{i\boldsymbol{k}'\cdot\boldsymbol{x}}}{|\boldsymbol{k} + \boldsymbol{k}'|^2 - \omega^2/c^2}\right) . \tag{3.12}$$

We seek $\boldsymbol{A}_\perp$. Substitute equation (3.12) into equation (3.6) to obtain, after some algebra:

$$\begin{aligned} A_{\perp,j}(\boldsymbol{x}, t) = \gamma \sum_{k=1}^{3} \Bigg\{ & \sum_{\boldsymbol{n}} \left[\frac{\omega^2}{c^2} \delta_{jk} - (k_j + qn_j)(k_k + qn_k)\right] \frac{e^{i(\boldsymbol{k}+q\boldsymbol{n})\cdot\boldsymbol{x}}}{|\boldsymbol{k} + q\boldsymbol{n}|^2 - \omega^2/c^2} \\ & - \int \frac{d^3k'}{q^3}\left[\frac{\omega^2}{c^2} \delta_{jk} - (k_j + k'_j)(k_k + k'_k)\right] \frac{e^{i(\boldsymbol{k}+\boldsymbol{k}')\cdot\boldsymbol{x}}}{|\boldsymbol{k} + \boldsymbol{k}'|^2 - \omega^2/c^2}\Bigg\} e^{-i\omega t} A_{\perp,k}(0, 0) , \end{aligned} \tag{3.13}$$

where we have defined the dimensionless polarizability

$$\gamma \equiv \frac{4\pi\alpha}{d^3} . \tag{3.14}$$

Since $\boldsymbol{P}_0 \parallel \boldsymbol{A}_\perp(0, 0)$, equation (3.13) yields the "mode equation"

$$\gamma \sum_{k=1}^{3} M_{jk} e_k = e_j , \tag{3.15}$$

where

$$M_{jk} \equiv \sum_{\boldsymbol{n}} \frac{v^2\delta_{jk} - (\beta_j + n_j)(\beta_k + n_k)}{|\boldsymbol{\beta} + \boldsymbol{n}|^2 - v^2} - \int d^3\boldsymbol{\beta}' \frac{v^2\delta_{jk} - (\beta_j + \beta'_j)(\beta_k + \beta'_k)}{|\boldsymbol{\beta} + \boldsymbol{\beta}'|^2 - v^2} , \tag{3.16}$$

$v \equiv \omega/qc$, $\boldsymbol{\beta} = \boldsymbol{k}/q$, and $\boldsymbol{e}$ is a unit vector defining the polarization (i.e., the direction of $\boldsymbol{P}_0$). For given γ, the mode equation (3.15) relates $\boldsymbol{\beta}$ and v, and therefore determines the dispersion relation for the lattice.

We now seek more tractable expressions for the sums and integrals appearing in the expression (3.16) for M_{ij}. In Appendix A we show that the off-diagonal elements may be written

$$M_{jk}(v, \boldsymbol{\beta}) = -\int_0^\infty dx\, e^{v^2 x} \frac{1}{4x^2} \frac{\partial}{\partial\beta_j} \frac{\partial}{\partial\beta_k} G(\boldsymbol{\beta}, x) \quad \text{for} \quad j \neq k \tag{3.17}$$

where

$$G(\boldsymbol{\beta}, x) \equiv g(\beta_1, x) g(\beta_2, x) g(\beta_3, x) \tag{3.18}$$

$$g(\beta, x) \equiv \sum_{n=-\infty}^{\infty} \exp[-x(\beta + n)^2] . \tag{3.19}$$

The diagonal terms may be written (see Appendix A)

$$M_{jj}(v, \boldsymbol{\beta}) = \int_0^\infty dx \left\{ e^{v^2 x} G(\boldsymbol{\beta}, x)\left[v^2 + \frac{\partial}{\partial x} \ln g(\beta_j, x)\right] - \left(\frac{\pi}{x}\right)^{3/2}\left(\frac{xv^2 - 1}{2x}\right)\right\} - \frac{4\pi^2}{3} v^3 i . \tag{3.20}$$

It is apparent from equations (3.17)–(3.20) that the mode equation (3.16) is, as expected, invariant under the replacement $\boldsymbol{\beta} \to \boldsymbol{\beta} + \boldsymbol{n}$, for arbitrary $\boldsymbol{n} = (i, j, k)$.

4. DISPERSION RELATION IN THE LONG-WAVELENGTH LIMIT

In principle, the M_{jk} can be evaluated for any finite $\boldsymbol{\beta}$ and v, and the mode equation (3.15) solved to find, for example, γ for given $\boldsymbol{\beta}$ and v. For application to the DDA we will be interested primarily in $|\beta| < 1$ and $v < 1$, since it is obvious that an array of point dipoles cannot adequately mimic a continuum target unless the lattice spacing is small compared to the wavelength. To this end we expand the M_{jk} in powers of β_j and ν. In Appendix B we show that

$$M_{jk}(\nu, \beta) = \left\{\frac{\nu^2\delta_{jk} - \beta_j\beta_k}{\beta^2 - \nu^2} + \frac{1}{3}\,\delta_{jk} + \delta_{jk}[c_1\nu^2 + c_2(\beta^2 - 3\beta_j^2)] + (1 - \delta_{jk})c_3\,\beta_j\beta_k - \delta_{jk}\,\frac{4\pi^2 i}{3}\,\nu^3 + O(\beta^4, \nu^4, \beta^2\nu^2)\right\} \tag{4.1}$$

(summation over repeated indices *not* implied). The coefficients c_1, c_2, and c_3 are

$$c_1 = \frac{2}{3}\int_0^\infty dx\left[g^3(0, x) - \left(\frac{\pi}{x}\right)^{3/2} - 1\right] = -5.9424219\ldots, \tag{4.2}$$

$$c_2 = \int_0^\infty dx\left\{\frac{1}{2}\,g(0, x)\left[\frac{\partial^2 g(\beta, x)}{\partial\beta^2}\right]_{\beta=0} \frac{\partial g(0, x)}{\partial x}\right\} = 0.5178819\ldots, \tag{4.3}$$

$$c_3 = \int_0^\infty dx\left\{1 - \frac{g(0, x)}{4x^2}\left[\frac{\partial^2 g(\beta, x)}{\partial\beta^2}\bigg|_{\beta=0}\right]^2\right\} = 4.0069747\ldots. \tag{4.4}$$

Given the dimensionless frequency ν, direction of propagation defined by unit vector $\boldsymbol{a}$, and polarization state defined by unit vector $\boldsymbol{e}$, we will use the "mode equation" (3.15) to determine the dipole polarizabilities α such that the lattice will propagate waves with $\boldsymbol{\beta} = m\nu\boldsymbol{a}$, where $m = \epsilon^{1/2}$ is the (complex) refractive index and $|\boldsymbol{a}| = 1$. We fix the propagation direction $\boldsymbol{a}$ and consider the limit $\nu^2 \ll 1$.We write

$$\gamma = \gamma^{(0)} + \gamma^{(1)} + O(\nu^4)\,, \tag{4.5}$$

$$M_{ij} = M_{ij}^{(0)} + M_{ij}^{(1)} + O(\nu^4)\,, \tag{4.6}$$

$$\boldsymbol{e} = \boldsymbol{e}^{(0)} + \boldsymbol{e}^{(1)} + O(\nu^4)\,, \tag{4.7}$$

where superscripts 0 and 1 designate the zero frequency limit and the leading order corrections:

$$M_{jk}^{(0)} = \frac{m^2 + 2}{3(m^2 - 1)}\,\delta_{jk} - \frac{m^2}{m^2 - 1}\,a_j a_k\,, \tag{4.8}$$

$$M_{jk}^{(1)} = \nu^2\delta_{jk}[c_1 + m^2c_2(1 - 3a_j^2)] + m^2\nu^2(1 - \delta_{jk})c_3\,a_j a_k - \frac{4\pi^2 i}{3}\,\delta_{jk}\,\nu^3\,. \tag{4.9}$$

To zeroth order we have

$$\gamma^{(0)}\sum_k M_{jk}^{(0)}e_k^{(0)} = e_j^{(0)}\,. \tag{4.10}$$

In the zero frequency limit we have $\boldsymbol{a}\cdot\boldsymbol{e}^{(0)} = 0$, and the solution is just the Clausius-Mossotti equation:

$$\gamma^{(0)} \equiv \frac{4\pi\alpha^{(0)}}{d^3} = \frac{3(m^2 - 1)}{m^2 + 2}\,. \tag{4.11}$$

The first-order equation is

$$\gamma^{(0)}\left\{\sum_{k=1}^{3}\,[M_{jk}^{(1)}e_k^{(0)} + M_{jk}^{(0)}e_k^{(1)}]\right\} + \gamma^{(1)}\sum_{k=1}^{3} M_{jk}^{(0)}e_k^{(0)} = e_j^{(1)}\,. \tag{4.12}$$

Contracting with $e_j^{(0)}$ yields (using $\sum_k e_k^{(0)}e_k^{(1)} = 0$, as required by $\boldsymbol{e}\cdot\boldsymbol{e} = 1$)

$$\gamma^{(1)} = -[\gamma^{(0)}]^2\sum_{j=1}^{3}\sum_{k=1}^{3} M_{jk}^{(1)}e_k^{(0)}e_j^{(0)}\,, \tag{4.13}$$

which yields (using $\sum_k a_k^{(0)}e_k^{(0)} = 0$)

$$\gamma \approx \gamma^{(0)}\left\{1 - \gamma^{(0)}\nu^2\left[c_1 + m^2c_2 - m^2(3c_2 + c_3)S - \frac{4\pi^2 i}{3}\,\nu\right]\right\}. \tag{4.14}$$

where

$$S(\boldsymbol{a}, \boldsymbol{e}) \equiv \sum_j (a_j e_j^{(0)})^2\,. \tag{4.15}$$

For ease of comparison with eq. (2.9), we replace (4.14) by

$$\alpha \approx \frac{\alpha^{(0)}}{1 + (\alpha^{(0)}/d^3)[(b_1 + m^2b_2 + m^2b_3\,S)(k_0\,d)^2 - (2/3)i(k_0\,d)^3]}\,, \tag{4.16}$$

or, removing the radiative reaction correction, we write

$$\alpha = \frac{\alpha^{(nr)}}{1 - (2/3)i(\alpha^{(nr)}/d^3)(k_0\,d)^3} \tag{4.17}$$

with

$$\alpha^{(nr)} = \frac{\alpha^{(0)}}{1 + (\alpha^{(0)}/d^3)[b_1 + m^2 b_2 + m^2 b_3 S](k_0 d)^2} , \quad (4.18)$$

$$b_1 = c_1/\pi = -1.8915316 , \quad (4.19)$$

$$b_2 = c_2/\pi = 0.1648469 , \quad (4.20)$$

$$b_3 = (3c_2 + c_3)/\pi = -1.7700004 , \quad (4.21)$$

with $\alpha^{(0)}$ given by equation (2.5). We see that the $O[(k_0 d)^2]$ correction term depends on the refractive index m and, through the quantity S, on the direction of propagation $\boldsymbol{a}$ and the polarization state $\boldsymbol{e}^{(0)}$.

The dependence on direction and polarization enters solely through the quantity $S \equiv \sum_j (a_j e_j^{(0)})^2$. We note that the allowed values of S range from 0 [e.g., for $\boldsymbol{a} = (1, 0, 0)$] to $\frac{1}{2}$ [e.g., for $\boldsymbol{a} \parallel (1, 1, 0)$ and $\boldsymbol{e} \parallel (1, -1, 0)$]. For randomly-oriented $\boldsymbol{a}$ and randomly oriented $\boldsymbol{e}^{(0)} \perp \boldsymbol{a}$, we show in Appendix C that

$$\langle S \rangle \equiv \left\langle \sum_{j=1}^{3} (a_j e_j^{(0)})^2 \right\rangle = \frac{1}{5} . \quad (4.21)$$

5. APPLICATION OF THE LDR TO THE DDA

We have found a prescription for choosing dipole polarizabilities $\alpha(k_0 d, m, \boldsymbol{a}, \boldsymbol{e})$ such that an infinite cubic lattice of point dipoles with lattice spacing d will propagate plane waves of frequency $\omega = k_0 c$ with wavevector $\boldsymbol{k} = m k_0 \boldsymbol{a}$ and polarization in the $\boldsymbol{e}$ direction (here $\boldsymbol{a}$ and $\boldsymbol{e}$ are unit vectors). Our prescription (4.18) is accurate to $O[(k_0 d)^3]$. While this result is for an infinite lattice, it seems reasonable to suppose that this may also be the "best" prescription for α such that a finite dipole array would mimic the absorption and scattering properties of a finite target of refractive index m (where the occupied lattice sites are selected to best mimic the target geometry). In the case of a finite target, there will be waves propagating in many different directions: the incident plane wave, plus the scattered radiation. Since the LDR depends on the wave direction $\boldsymbol{a}$ and polarization $\boldsymbol{e}$, we must specify $\boldsymbol{a}$ and $\boldsymbol{e}$; we will take $\boldsymbol{a}$ and $\boldsymbol{e}$ to be those for the incident plane wave. We will also consider an "isotropized" version of the LDR, where we replace $S(\boldsymbol{a}, \boldsymbol{e})$ in eq. (4.18) by the average value $\langle S \rangle = \frac{1}{5}$. This will be referred to as the "isotropized lattice dispersion relation" (ILDR).

As a test of the different prescriptions for α, we will calculate scattering and absorption by dipole arrays intended to approximate homogeneous spheres. This shape is chosen because it is possible to use Mie scattering theory to compute the exact solution for comparison with the DDA results. Except for the choice of the nonradiative polarizabilities $\alpha^{(nr)}$, the DDA calculations were carried out following Draine (1988), with Fast Fourier Transforms used to evaluate the left-hand side of equation (2.4) (Goodman, Draine, & Flatau 1991).[5,6]

We examine five different cases of the refractive index: $m = 1.1 + 0.001i$, $m = 1.33 + 0.01i$, $m = 1.7 + 0.1i$, $m = 2 + 1i$, and $m = 3 + 4i$. These five cases span a range of material properties, from weakly polarizable and very weakly absorbing ($m = 1.1 + 0.001i$, $\epsilon = 1.21 + 0.0022i$) to very highly absorptive ($m = 3 + 4i$, $\epsilon = -7 + 24i$).

In our calculations we use arrays of $N = 17904$ dipoles (chosen to be the lattice sites located within a sphere of diameter $32.49d$, with center located between lattice sites). The dipole geometry is shown in Figure 1, where each point dipole is represented by a small sphere of diameter d. The effective radius of this target is $a_{\text{eff}} \equiv (3N/4\pi)^{1/3} d = 16.23d$. Because the occupied lattice sites are contained within a $2^5 \times 2^5 \times 2^5$ region of the lattice, the FFT algorithm is particularly efficient.

Because the dipole array is of course not spherically symmetric, the scattering and absorption properties depend upon the direction of propagation $\boldsymbol{k}_0$. The results in Figures 2–6 are for $\boldsymbol{k}_0 \parallel (1, 1, 1)$ and $\boldsymbol{e} \parallel (2, -1, -1)$ in the "target frame." Although the $N = 17904$ pseudosphere is not spherically symmetric, the reflection symmetries of the target ensure that the absorption and scattering cross sections do not depend on the incident polarization $\boldsymbol{e}$ for $\boldsymbol{k}_0 \parallel (1, 1, 1)$ [note that $S(\boldsymbol{a}, \boldsymbol{e}) = \frac{1}{3}$ independent of $\boldsymbol{e}$ for $\boldsymbol{a} \parallel (1, 1, 1)$]. For each refractive index m, we obtain DDA scattering solutions for four different prescriptions for the polarizability α:

1. The CMRR prescription (eq. [2.7]) of Draine (1988).
2. The DGF/VIEF prescription (eq. [2.9]) of Goedecke & O'Brien (1988) and Hage & Greenberg (1990).
3. The Lattice Dispersion Relation (LDR) prescription (4.18) with $S(\boldsymbol{a}, \boldsymbol{e})$ evaluated for the incident direction and polarization.
4. The "Isotropized" Lattice Dispersion Relation (ILDR) with $S = \frac{1}{5}$ in equation (4.18).

In Figures 2–6 we show the fractional error in the scattering and absorption efficiencies $Q_{\text{sca}} = C_{\text{sca}}/\pi a_{\text{eff}}^2$ and $Q_{\text{abs}} = C_{\text{abs}}/\pi a_{\text{eff}}^2$, where C_{sca} and C_{abs} are the cross sections for scattering and absorption. Results are shown as functions of $|m| k_0 d$; at the top of each graph we show the corresponding values of the usual "scattering parameter" $x = k_0 a_{\text{eff}} = 2\pi a_{\text{eff}}/\lambda$. In Figures 2–6 we see that in the "static" limit $k_0 d \to 0$ all four prescriptions converge to the same result; the result differs from the exact solution for a sphere because the $N = 17904$ array of occupied sites is only an approximation to a sphere. As $|m| k_0 d$ increases, we see that the four prescriptions give different results. We shall concentrate on the regime $|m| k_0 d \lesssim 0.5$, since we shall see below that for larger values of $|m| k_0 d$ the DDA solutions do not provide accurate differential scattering cross sections.

[5] On the Sun 4/50 Sparcstation IPX used for these calculations, one complex conjugate gradient iteration for the $N = 17904$ dipole pseudosphere required 90 cpu s. The number of iterations required to converge to a solution depends on m, $x = k_0 a_{\text{eff}}$, $\boldsymbol{a}$, and $\boldsymbol{e}$. For the scattering problem of Fig. 7 ($m = 1.33 + 0.01i$, $x = 4$) $\sim$14 iterations were required per solution. The scattering problem of Fig. 8 ($m = 2 + i$, $x = 3$) required $\sim$26 iterations per solution.

[6] The FORTRAN program DDSCAT.4b used for these calculations is available upon request. Direct queries to Internet address "draine@astro.princeton.edu."

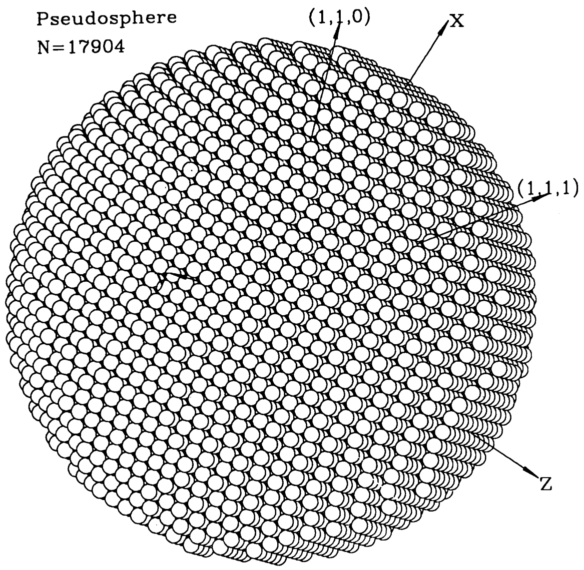

FIG. 1

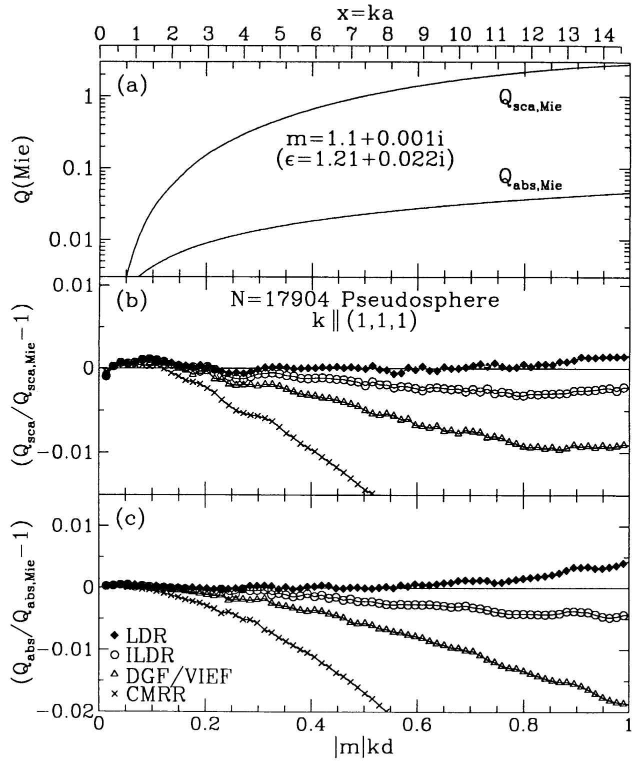

FIG. 2

FIG. 1.—Pseudosphere composed of $N = 17904$ point dipoles. The effective radius is $a_{\rm eff} = (3N/4\pi)^{1/3}d = 16.23d$, where d is the lattice spacing.

FIG. 2.—(*a*) Scattering and absorption efficiency factors $Q_{\rm sca}$ and $Q_{\rm abs}$ for a sphere of refractive index $m = 1.1 + 0.001i$ ($\epsilon = 1.21 + 0.0022i$, $|m - 1| = 0.10$, $|\epsilon - 1| = 0.21$). (*b*) Fractional error in computed value of $Q_{\rm sca}$ for the $N = 17904$ pseudosphere of Fig. 1. (*c*) Fractional error in computed value of $Q_{\rm abs}$ for the $N = 17904$ pseudosphere. Results are shown for four different prescriptions for the dipole polarizabilities: CMRR (Clausius-Mossotti plus radiative reaction; Draine 1988); DGF/VIEF (digitized Green's function/volume integral equation formulation; Goedecke & O'Brien 1988, Hage, Greenberg, & Wang 1990); and LDR and ILDR (lattice dispersion relation and isotropized lattice dispersion relation; this paper). Results are shown as functions of $|m|k_0 d$, where m is the refractive index, k_0 is the wavevector in vacuo, and d is the lattice spacing. Also shown (*top axis*) is $x = k_0 a_{\rm eff}$. For this case it is apparent that the LDR prescription provides the best accuracy.

Inspection of Figures 2–6, with emphasis on the regions $|m|k_0 d \lesssim 0.5$, yields the following conclusions:

1. We confirm the conclusion of Hage & Greenberg (1990): the DGF/VIEF method generally gives more accurate results than the CMRR method.
2. For $|\epsilon - 1| \lesssim 3$, or $|m - 1| \lesssim 1$ (Figs. 2–4) the LDR prescription provides remarkably accurate results for $|m|k_0 d \lesssim 0.5$; it is clearly superior to the other prescriptions considered. The ILDR prescription, though not as good as the LDR, is nevertheless preferable to the DGF/VIEF prescription.
3. For $|\epsilon - 1| \gtrsim 4$, or $|m - 1| \gtrsim 1$, (Figs. 5 and 6) the LDR, ILDR, and DGF/VIEF methods are of comparable accuracy. For $|\epsilon - 1| = 4.47$ ($|m - 1| = 1.41$; Fig. 5) the DDA with $N = 17904$ permits calculation of $Q_{\rm sca}$ and $Q_{\rm abs}$ to within a few percent for $|m|k_0 d \lesssim 0.5$, but for $|\epsilon - 1| = 25.3$ ($|m - 1| = 4.47$; Fig. 6) the errors, particularly in $Q_{\rm abs}$, are quite large ($\sim$20%) even for $|m|k_0 d = 0.3$.

When $|m - 1|$ is large the continuum material is effective at "screening" the external field: in the limit $|m - 1| \to \infty$ the internal field generated by the polarization would exactly cancel the incident field, so that the continuum material in the interior of the target would be subjected to zero field. In the case of a discrete dipole array, the dipoles in the interior will also be effectively shielded (although probably not quite as thoroughly) but the dipoles located on the target surface are not fully shielded and, as a result, absorb energy from the external field at an excessive rate: this is why the DDA so greatly overestimates $Q_{\rm abs}$ in Figure 6, even in the "static" limit $k_0 \to 0$. The errors can of course be reduced to any desired level by increasing the number N of dipoles, thereby minimizing the fraction $\sim N^{-1/3}$ of the dipoles which are at surface sites, but very large values of N are required when $|m|$ is very large. It is apparent that the DDA method is not particularly well-suited for target materials with very large $|m|$ (e.g., conducting materials in the far-infrared).

As discussed above, the DDA results in principle should depend on the direction and polarization of the incident radiation. To see the magnitude of this effect, in Figures 7 and 8 we show results of DDA calculations for different incident directions. The propagation vector for the radiation is taken to be

$$\boldsymbol{a} = (1, 0, 0) \cos\theta + (0, 1, 1)2^{-1/2} \sin\theta \qquad (5.1)$$

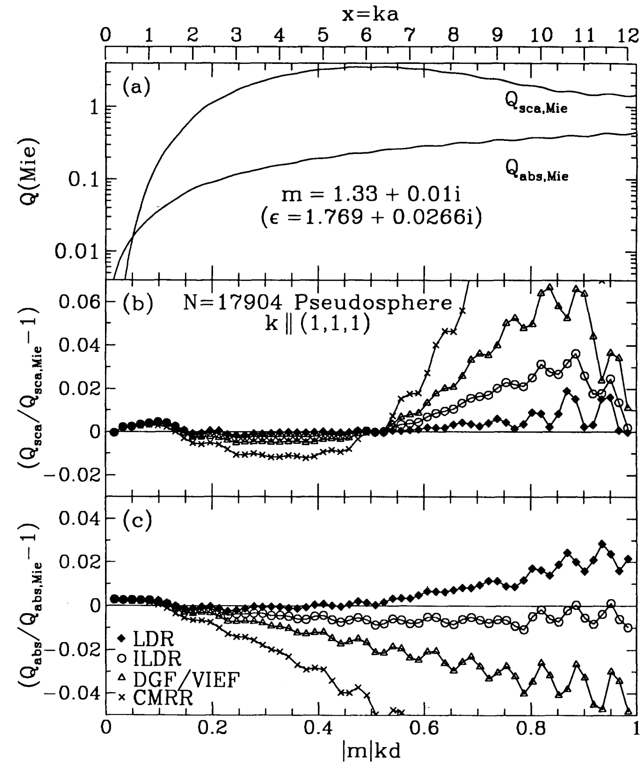

FIG. 3

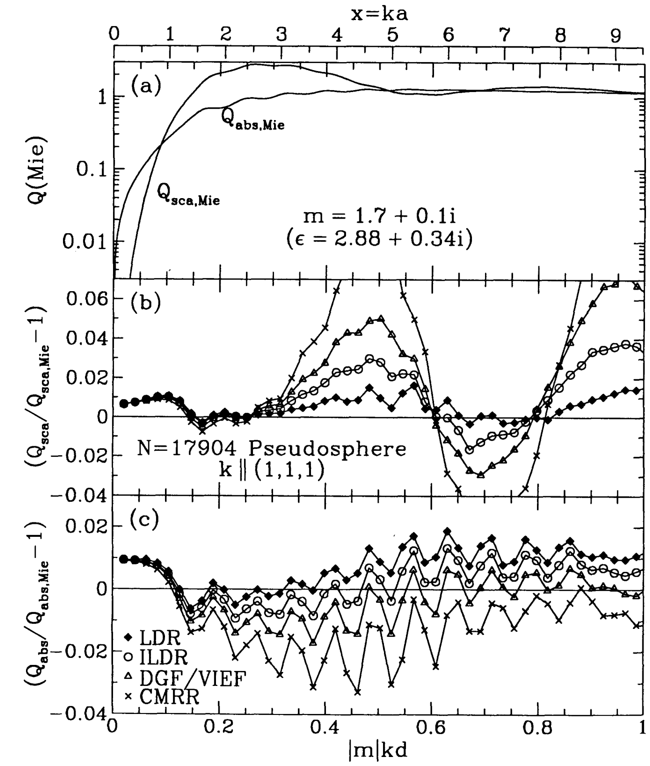

FIG. 4

FIG. 3.—Same as Fig. 2, but for $m = 1.33 + 0.01i$ ($\epsilon = 1.769 + 0.0266$, $|m - 1| = 0.330$, $|\epsilon - 1| = 0.769$). For this case the LDR prescription is clearly superior for $|m|k_0 d \lesssim 0.5$.

FIG. 4.—Same as Fig. 2, but for $m = 1.7 + 0.1i$ ($\epsilon = 2.88 + 0.34i$, $|m - 1| = 0.707$, $|\epsilon - 1| = 1.91$). For this case the LDR prescription is clearly superior for $|m|k_0 d < 0.5$.

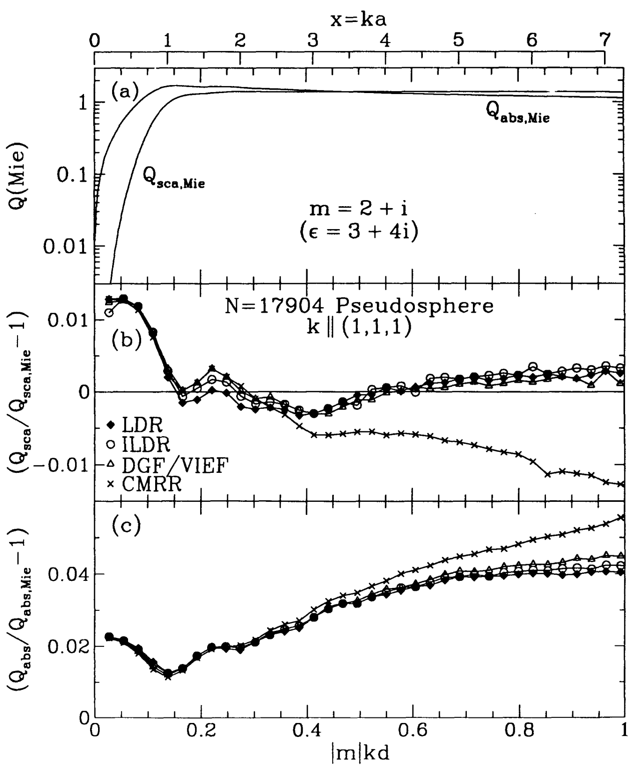

FIG. 5

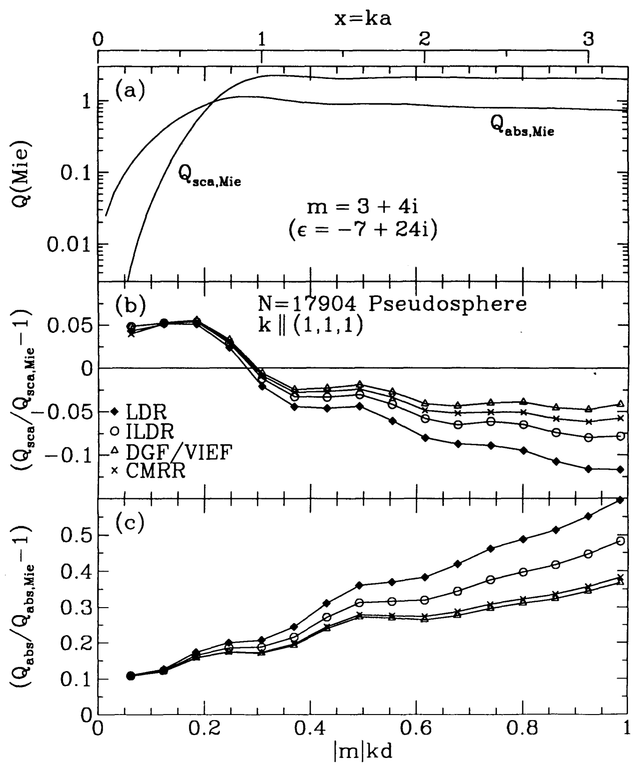

FIG. 6

FIG. 5.—Same as Fig. 2, but for $m = 2 + i$ ($\epsilon = 3 + 4i$, $|m - 1| = 1.414$, $|\epsilon - 1| = 4.472$). For this case the DGF/VIEF, ILDR, and LDR prescriptions provide comparable overall accuracy.

FIG. 6.—Same as Fig. 2, but for $m = 3 + 4i$ ($\epsilon = -7 + 24i$, $|m - 1| = 4.472$, $|\epsilon - 1| = 25.30$). For this case the DDA methods do a fair job in calculation of Q_{sca} (errors $\lesssim 5\%$ for $|m|k_0 d < 0.5$) but substantially overestimate Q_{abs}. Accurate DDA calculations for targets with large $|\epsilon - 1|$ require very large N.

and the results shown are for the polarization state

$$e = (0, 1, 1)2^{-1/2} \cos \theta - (1, 0, 0) \sin \theta . \quad (5.2)$$

In Figure 7 we show the fractional error in the scattering and absorption cross sections as functions of θ for $m = 1.33 + 0.01i$ and $x = 4$ ($|m| k_0 d = 0.328$) Note that the CMRR, DGF/VIEF, and ILDR methods all result in errors which depend on the direction of incidence. By contrast, the LDR method has very small errors, and these errors are nearly independent of the direction of incidence! We conclude that the LDR method appears to correctly compensate for the anisotropic response of the dipole lattice. For this case the ILDR method appears, as expected, to give the correct average over incident directions, but the LDR method has far smaller rms errors, and is clearly superior.

In Figure 8 we show the angle-dependent errors for $m = 2 + i$ and $x = 3$ ($|m| k_0 d = 0.413$). In this case all methods appear to be about equally good; all show similar angle-dependent errors. Why is the LDR method not better here? We attribute this to the fact that for scattering by this finite target the full scattering solution involves radiation propagating in many different directions within the target, not just in the original incident direction. Since the polarizabilities α in the LDR method were "optimized" only for radiation propagating along the direction of incidence and with the polarization of the incident radiation [as well as for other directions and polarizations having the same values of $\sum_j (a_j e_j)^2$] it follows that the angle-dependent correction terms in the LDR method will be inappropriate when the field within the target includes substantial components in addition to the incident field. This would account for the fact that the LDR method achieves high accuracy for a dielectric material with modest refractive index ($m = 1.33 + 0.01i$) but does not do much better than the DGF/VIEF or ILDR methods for a material with a large dielectric constant ($m = 2 + i$).

Finally, in Figure 9 we show that the different DDA solutions allow accurate calculation of differential scattering cross sections for $|m| k_0 d \lesssim 0.5$. Shown are differential scattering cross sections for $\theta = 180°$ backscattering as functions of $|m| k_0 d$ for $m = 1.33 + 0.01i$ and $m = 2 + i$. We see that all four methods for prescribing the polarizabilities give about equally good results for differential scattering cross sections: the errors are small for $|m| k_0 d \lesssim 0.5$ but become substantial as $|m| k_0 d$ is increased further.

6. CONCLUSIONS

We have formally solved the problem of propagation of plane electromagnetic waves on an infinite lattice of polarizable points with lattice spacing d; in effect, the Clausius-Mossotti relation has been extended to the case $\omega d/c \neq 0$. This "lattice dispersion relation" (LDR) is then used, in the limit $k_0 d \ll 1$, to obtain a prescription for choosing the point polarizabilities α such that the lattice will have the same dispersion relation as a continuum material of complex refractive index $m = \epsilon^{1/2}$: the resulting prescription is given in equations (4.17)–(4.18).

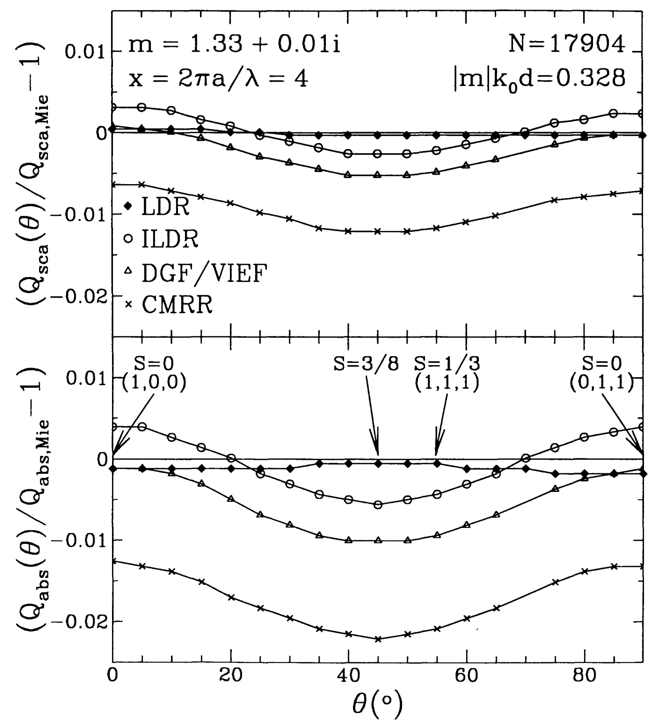

FIG. 7

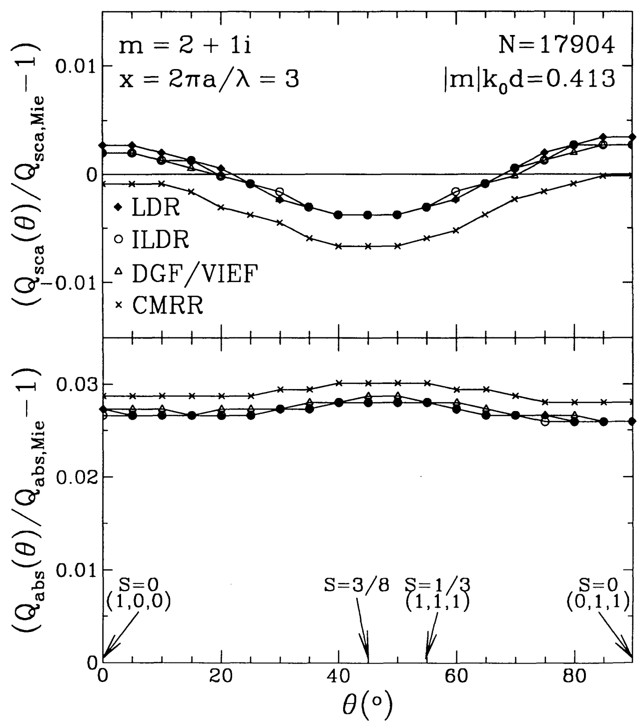

FIG. 8

FIG. 7.—Fractional errors in calculation of Q_{sca} and Q_{abs} for $N = 17904$ pseudosphere with $m = 1.33 + 0.01i$ and $x = k_0 a_{eff} = 4$, as a function of the direction of incidence of the radiation (with direction and polarization given by eqs. [5.1]–[5.2]). For this case the LDR method appears to properly correct for the effects of varying direction of incidence. The quantity $S(\boldsymbol{a}, \boldsymbol{e})$ defined by eq. (4.15) is given for selected directions.

FIG. 8.—Same as Fig. 7, but for $m = 2 + i$ and $x = 3$. For this case the LDR, ILDR, and DGF/VIEF methods give quite similar results (as expected from Fig. 5).

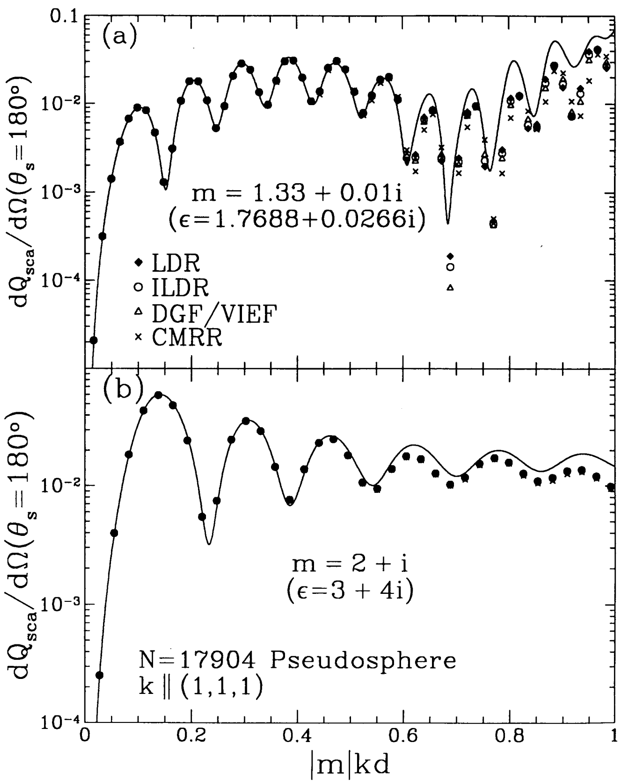

FIG. 9.—Differential cross section for backscattering. Solid line is exact result for sphere from Mie theory; symbols show results of DDA calculations for different prescriptions for polarizability α. Results are shown for $N = 17904$ pseudosphere with (a) $m = 1.33 + 0.01i$; (b) $m = 2 + i$. Small differences in accuracy for $|m| k_0 d < 0.5$ are not visible. It is apparent that reasonably accurate results for differential scattering cross sections are obtained for $|m| k_0 d \lesssim 0.5$.

The resulting polarizabilities include terms of $O[(k_0 d)^2]$ in addition to an $O[(k_0 d)^3]$ radiative reaction correction. The $O[(k_0 d)^2]$ correction depends explicitly on the orientation of the wave propagation vector and polarization relative to the lattice.

The motivation for this study was to improve the accuracy of DDA calculations for scattering and absorption. We find that the LDR prescription (eq. [4.18]) for assigning dipole polarizabilities substantially improves the accuracy of DDA calculations for spheres composed of materials with $|\epsilon - 1| \lesssim 3$. For $|\epsilon - 1| \approx 5$ the LDR prescription is still marginally superior to the other prescriptions considered. For $|\epsilon - 1| \gtrsim 5$ the LDR and DGF/VIEF prescriptions for assigning dipole polarizabilities appear to be about equally good.

Although the scattering calculations presented here have been restricted to homogeneous spheres, we expect the DDA to be an excellent tool for calculation of scattering and absorption by irregular and inhomogeneous targets, provided only that (1) $|m| k_0 d \lesssim 0.5$, where d is the interdipole spacing; (2) $|\epsilon - 1| \lesssim 10$; and (3) d is small compared to all structural scales in the target, so that the dipole array may faithfully represent the target geometry. For very large values of the refractive index m the accuracy of the DDA suffers; using the LDR prescription for α the DDA gives fair accuracy for scattering but poorer results for absorption, and it is necessary to restrict use to somewhat smaller values of $|m| k_0 d$ than was necessary for smaller values of $|m|$. When the dielectric constant is very large, other methods, such as the "T-matrix" or "extended boundary condition method" (e.g., Mugnai & Wiscombe 1989) may be preferable.

We thank Piotr Flatau for helpful comments. This research was supported in part by NSF grant AST-9017082 and NASA grant NAGW-1973 to B. T. D., and by a David and Lucille Packard Foundation Fellowship and a Sloan Foundation Fellowship to J. G.

APPENDIX A

Here we show how the infinite triple sums and integrals that appear in the mode matrix (3.16) can be converted to one-dimensional integrals.

For $j \neq k$,

$$-\frac{(\beta_j + n_j)(\beta_k + n_k)}{|\boldsymbol{\beta} + \boldsymbol{n}|^2 - \nu^2} = -\frac{\partial}{\partial \beta_j}\frac{\partial}{\partial \beta_k}\int_0^\infty dx\, \frac{1}{4x^2} \exp\left[x(\nu^2 - |\boldsymbol{\beta} + \boldsymbol{n}|^2)\right] , \tag{A1}$$

provided that

$$\nu^2 < |\boldsymbol{\beta} + \boldsymbol{n}|^2 , \tag{A2}$$

which is guaranteed if $\omega/c < k$ (as expected for propagation in a medium of refractive index greater than unity) and $kd < \pi$.

Now,

$$\sum_{\boldsymbol{n}} \exp(-x|\boldsymbol{\beta}+\boldsymbol{n}|^2) = \prod_{l=1}^{3}\left\{\sum_{n_l=-\infty}^{\infty} \exp[-x(\beta_l+n_l)^2]\right\} \equiv \prod_{l=1}^{3} g(\beta_l, x) . \tag{A3}$$

This establishes formula (3.17) for M_{jk}, since the integral over $\boldsymbol{\beta}'$ in equation (3.16) vanishes for $j \neq k$ by symmetry.

We remark that $g(\beta, x)$ can be expressed in the alternate forms

$$g(\beta, x) = \left(\frac{\pi}{x}\right)^{1/2} \theta_3(\pi\beta, e^{-\pi^2/x}) \equiv \left(\frac{\pi}{x}\right)^{1/2} \sum_{n=-\infty}^{\infty} e^{-n^2\pi^2/x} \cos(2\pi n\beta) , \tag{A4}$$

where θ_3 is an elliptic θ function (see Abramowitz & Stegun 1972, § 16.27.3). The equivalence of the two series for g can be proved by considering the integral

$$\frac{1}{2\pi i}\int_C \exp[-x(z+\beta)^2] \cot z\, dz ,$$

along an appropriate contour C enclosing the entire real axis, and evaluating the integral in two ways: (1) by summing the residues at the poles of cot$z$; (2) by expanding cot$z$ in powers of $e^{\pm iz}$ and integrating term by term. The series (3.19) converges rapidly for $x > 1$, while equation (A4) converges rapidly for $x < \pi^2$. As $x \to 0^+$, $g(\beta, x)$ diverges like $x^{-1/2}$ because of the $n = 0$ term in the second sum; the rest diminishes faster than any power of x.

Applying identities similar to equation (A1) to the sum and the integral in equation (3.16), we have

$$M_{jj} = \int_0^\infty dx\, e^{v^2x}\left\{G(\boldsymbol{\beta}, x)\left[v^2 + \frac{1}{g(\beta_j, x)}\frac{\partial}{\partial x} g(\beta_j, x)\right] - \left(\frac{\pi}{x}\right)^{3/2}\left(v^2 - \frac{1}{2x}\right)\right\} . \tag{A5}$$

The terms proportional to $G(\beta, x)$ give no trouble at large x as long as equation (A2) is satisfied for all $\boldsymbol{n}$, but the remainder of the integrand in (A5) is divergent at large x because of the factor exp (v^2x). This divergence reflects the pole in the denominator of the integral part of equation (3.16) (which in turn reflects the dispersion relation in vacuo). Because the pole occurs inside an integral over $\boldsymbol{\beta}'$, it gives rise to a branch cut in the complex v^2 plane along the positive real axis. To make sense of equation (A5), therefore, we define it by analytic continuation from the *negative real* v^2 axis (or equivalently, the positive imaginary ω axis), where the integral over x is well defined. The entire cut v^2 plane corresponds to Im $(\omega) > 0$ and hence to the use of retarded potentials for the solution of equation (3.2).

To carry out this analytic continuation, we first rewrite equation (A5):

$$M_{jj} = \int_0^\infty dx\left\{e^{v^2x}G(\boldsymbol{\beta}, x)\left[v^2 + \frac{\partial}{\partial x}\ln g(\beta_j, x)\right] - \left(\frac{\pi}{x}\right)^{3/2}\left(\frac{xv^2-1}{2x}\right)\right\} - R(v^2) , \tag{A6}$$

where

$$R(v^2) \equiv \int_0^\infty dx\, \frac{\pi^{3/2}}{2x^{5/2}}\left[(2v^2x-1)e^{v^2x} - v^2x + 1\right] . \tag{A7}$$

The integral for $(M_{jj} + R)$ is now well defined, provided

$$\mathrm{Re}\,(v^2) \leq \min_{\boldsymbol{n}} |\boldsymbol{\beta}+\boldsymbol{n}|^2 . \tag{A8}$$

In fact, the only singularities of $M_{jj}(v, \boldsymbol{\beta}) + R(v^2)$ are simple poles at the points $v^2 = |\boldsymbol{\beta}+\boldsymbol{n}|^2$.

The bracketed part of the integrand in (A7) is $\propto x^2$ as $x \to 0$, so the integrand is integrably singular as $x \to 0$. With v on the positive imaginary axis, the integral is also convergent as $x \to \infty$, and we find

$$R(v^2) = \frac{4\pi^2}{3} iv^3 . \tag{A9}$$

Analytic continuation now justifies the use of this result throughout the upper half v plane. The remainder (A9) represents the radiation reaction field evaluated at $\boldsymbol{x} = 0$, which is the nonsingular part of $\boldsymbol{A}_{\mathrm{self}}(0, t)$.

APPENDIX B

Here we derive the mode matrix $M_{jk}(v, \boldsymbol{\beta})$ to $O(v^2, \beta^2)$, assuming $v \sim \beta \ll 1$. Noting that $g(\beta, x) \approx \exp(-\beta^2 x)$ as $x \to \infty$, let us write

$$\begin{aligned} g(\beta, x) &= g_c(\beta, x) + \Delta g(\beta, x) , \qquad & g_c(\beta, x) &\equiv \exp(-\beta^2 x) , \\ G(\boldsymbol{\beta}, x) &= G_c(\boldsymbol{\beta}, x) + \Delta G(\boldsymbol{\beta}, x) , \qquad & G_c(\boldsymbol{\beta}, x) &\equiv \exp(-|\boldsymbol{\beta}|^2 x) , \end{aligned} \tag{B1}$$

where the subscript "c" stands for "continuum."

To zeroth order in Δ, the integrands of equations (3.17) and (3.20) behave like $\exp[x(v^2 - \boldsymbol{\beta}^2)]$ as $x \to \infty$, and

$$M_{jk}(v, \boldsymbol{\beta}) \approx M^c_{jk}(v, \boldsymbol{\beta}) = -\frac{v^2\delta_{jk} - \beta_j\beta_k}{v^2 - |\boldsymbol{\beta}|^2}, \tag{B2}$$

which is just the $\boldsymbol{n} = 0$ term in the sum (3.16).

We next consider $\Delta M_{jk} \equiv M_{jk} - M^c_{jk}$ at $v = 0 = \boldsymbol{\beta}$. One expects the off-diagonal terms ($j \neq k$) to vanish, because when $\beta = 0$, the only preferred directions are the lattice axes. To verify this explicitly, notice from (B1) and (A4) that both $g_c(\beta, x)$ and $g(\beta, x)$ are even functions of β, whence $\partial g_c/\partial\beta = \partial\Delta g/\partial\beta = 0$ at $\beta = 0$, and therefore

$$\Delta M_{jk}(0, 0) = -\int_0^\infty \frac{dx}{4x^2}\,\Delta\left[g(\beta_i, x)\frac{\partial g}{\partial\beta_j}(\beta_j, x)\frac{\partial g}{\partial\beta_k}(\beta_k, x)\right]_{\beta=0} = 0\,, \quad i \neq j \neq k, \quad i \neq k\,. \tag{B3}$$

For $j = k$, on the other hand, equation (3.20) yields

$$\Delta M_{jj}(0, 0) = \int_0^\infty dx\left[g^2(0, x)\frac{\partial g}{\partial x}(0, x) + \frac{\pi^{3/2}}{2x^{5/2}}\right] = \frac{1}{3}\left[g^3(0, x) - \left(\frac{\pi}{x}\right)^{3/2}\right]_{x=0}^{\infty} = \frac{1}{3}\,. \tag{B4}$$

This justifies the term $\frac{1}{3}\delta_{jk}$ in equation (4.1).

The coefficient of v^2 in $\Delta M_{jk}(v, 0)$ vanishes for $j \neq k$ by the same symmetry argument given above. For $j = k$ we have, using equation (3.20),

$$\begin{aligned} c_1 = \left.\frac{\partial\Delta M_{jj}}{\partial v^2}\right|_{v^2=0,\boldsymbol{\beta}=0} &= \int_0^\infty dx\left[G(0, x) - 1 + xg^2(0, x)\frac{\partial g}{\partial x}(0, x) - \frac{1}{2}\left(\frac{\pi}{x}\right)^{3/2}\right] \\ &= \int_0^\infty dx\left\{\frac{x}{3}\frac{d}{dx}\left[g^3(0, x) - \left(\frac{\pi}{x}\right)^{3/2} - 1\right] + G(0, x) - \left(\frac{\pi}{x}\right)^{3/2} - 1\right\} \\ &= \frac{2}{3}\int_0^\infty dx\left[G(0, x) - \left(\frac{\pi}{x}\right)^{3/2} - 1\right], \end{aligned} \tag{B5}$$

where the "-1" comes from "$-G_c(0, x)$," and we have passed from the second to the third line by integrating by parts (the combination in square brackets on the second line is finite as $x \to 0$ and is integrable as $x \to \infty$).

Next, consider the coefficient of β_k^2 in the diagonal element ΔM_{jj}. For $k \neq j$, it follows rather directly from equation (3.20) that

$$c_2 = \frac{1}{2}\left.\frac{\partial^2\Delta M_{jj}}{\partial\beta_k^2}\right|_{v^2=0,\boldsymbol{\beta}=0} = \frac{1}{2}\int_0^\infty dx\, g(0, x)\left[\frac{\partial^2 g(\beta_k, x)}{\partial\beta_k^2}\right]_{\beta_k=0}\frac{\partial g}{\partial x}(0, x)\,, \tag{B6}$$

which is equation (4.3). On the other hand, the trace of ΔM_{jk} is independent of $\boldsymbol{\beta}$ at $v^2 = 0$:

$$\sum_j \Delta M_{jj}(0, \boldsymbol{\beta}) = \int_0^\infty dx\left\{\frac{\partial}{\partial x}\left[G(\boldsymbol{\beta}, x) - e^{|\boldsymbol{\beta}|^2x}\right] + \frac{3}{2}\frac{\pi^{3/2}}{x^{5/2}}\right\} = \left[G(\boldsymbol{\beta}, x) - e^{|\boldsymbol{\beta}|^2x} - \left(\frac{\pi}{x}\right)^{3/2}\right]_{x=0}^{\infty} = 1\,. \tag{B7}$$

Hence if the coefficient of β_k^2 and β_l^2 in ΔM_{jj} is c_2 ($j \neq k \neq l, j \neq l$), the coefficient of β_j^2 must be $-2c_2$.

Finally, c_3 follows from equation (3.17) for $j \neq k$:

$$c_3 = \left.\frac{\partial^2\Delta M_{jk}}{\partial\beta_j\beta_k}\right|_{v^2=0,\boldsymbol{\beta}=0} = -\int_0^\infty dx\,\frac{1}{4x^2}\left[\frac{\partial^2}{\partial\beta_j^2}\frac{\partial^2}{\partial\beta_k^2}\Delta G(\boldsymbol{\beta}, x)\right]_{\boldsymbol{\beta}=0}, \tag{B8}$$

which leads directly to equation (4.4).

APPENDIX C

Let the general propagation vector $\boldsymbol{a}$ and polarization vector $\boldsymbol{e}^{(0)}$ be given by

$$\boldsymbol{a} = (\cos\theta, \sin\theta\cos\phi, \sin\theta\sin\phi) \tag{C1}$$

$$\boldsymbol{e}^{(0)} = [\sin\theta\cos\psi, (\sin\phi\sin\psi - \cos\theta\cos\phi\cos\psi), (-\cos\phi\sin\psi - \cos\theta\sin\phi\cos\psi)] \tag{C2}$$

where the angle $0 \leq \psi \leq 2\pi$ specifies the polarization state. Then

$$\begin{aligned} S \equiv \sum_{j=1}^{3}(a_j e_j^{(0)})^2 &= \sin^2\theta\cos^2\theta\cos^2\psi(1 + \cos^4\phi + \sin^4\phi) + 2\sin^2\theta\sin^2\phi\cos^2\phi\sin^2\psi \\ &\quad + 2\sin^2\theta\cos\theta\sin\phi\cos\phi\sin\psi\cos\psi(\sin^2\phi - \cos^2\phi)\,. \end{aligned} \tag{C3}$$

Averaging over ψ we obtain

$$\langle S\rangle_\psi = \tfrac{1}{2}\sin^2\theta\cos^2\theta(1 + \cos^4\phi + \sin^4\phi) + \sin^2\theta\sin^2\phi\cos^2\phi\,. \tag{C4}$$

Averaging further over ϕ we have

$$\langle S \rangle_{\psi\phi} = \tfrac{7}{8} \sin^2 \theta \cos^2 \theta + \tfrac{1}{8} \sin^2 \theta \,, \tag{C5}$$

and a final average over $\cos \theta$ yields

$$\langle S \rangle_{\psi\phi\theta} = \tfrac{1}{5} \,. \tag{C6}$$

REFERENCES

Abramowitz, M., & Stegun, I. A. 1972, Handbook of Mathematical Functions (Washington, DC: US GPO)
Draine, B. T. 1988, ApJ, 333, 848
Goedecke, G. H., & O'Brien, S. G. 1988, Appl. Opt., 28, 2431
Goodman, J. J., Draine, B. T., & Flatau, P. J. 1991, Opt. Lett., 16, 1198
Hage, J. I., & Greenberg, J. M. 1990, ApJ, 361, 251
Hage, J. I., Greenberg, J. M., & Wang, R. T. 1991, Appl. Opt., 9, 1141
Hawkins, I., & Wright, E. L. 1991, in Extreme Ultraviolet Astronomy, ed. R. F. Malina & S. Bowyer (New York: Pergamon), 333
Jackson, J. D. 1975, Classical Electrodynamics (New York: Wiley)
Kozasa, T., Blum, J., & Mukai, T. 1992, A&A, 263, 423
Livesay, D. E., & Chen, K. 1974, IEEE Trans. Microwave Theory & Techniques, MTT-22, 1273
Mugnai, A., & Wiscombe, W. J. 1989, Appl. Opt., 28, 3061
Ohtaka, K. 1979, Phys. Rev. B, 19, 5057
Purcell, E. M., & Pennypacker, C. R. 1973, ApJ, 186, 705
Shapiro, P. R. 1975, ApJ, 201, 151
Waterman, P. C., & Pedersen, N. E. 1986, J. Appl. Phys. 59, 2609
West, R. A. 1991, Appl. Opt., 30, 5316
West, R. A., Orton, G. S., Draine, B. T., & Hubbell, E. A. 1989, Icarus, 80, 220
Wright, E. L. 1988, Nature, 366, 227